ACS APPLIED MATERIALS & INTERFACES

Forum Article

www.acsami.org

Tuning the Interplay between Selectivity and Permeability of ZIF-7 Mixed Matrix Membranes

Bassem A. Al-Maythalony,*[,†] Ahmed M. Alloush,[†] Muhammed Faizan,[†] Hatim Dafallah,[†] Mohammed A. A. Elgzoly,[†] Adam A. A. Seliman,[†] Amir Al-Ahmed,[†] Zain H. Yamani,[‡] Mohamed A. M. Habib,[†] Kyle E. Cordova,[‡,§,∥] and Omar M. Yaghi*[,†,‡,§,∥]

[†]King Abdulaziz City for Science and Technology−Technology Innovation Center on Carbon Capture and Sequestration (KACST-TIC on CCS), King Fahd University of Petroleum and Minerals, Dhahran 31261, Saudi Arabia

[‡]Center for Research Excellence in Nanotechnology (CENT), King Fahd University of Petroleum and Minerals, Dhahran 31261, Saudi Arabia

[§]Department of Chemistry, Kavli Energy NanoSciences Institute at Berkeley, and Berkeley Global Science Institute, University of California—Berkeley, Berkeley, California 94720, United States

[∥]Materials Sciences Division, Lawrence Berkeley National Laboratory, Berkeley, California 94720, United States

Supporting Information

ABSTRACT: Nanoparticles of zeolitic imidazolate framework-7 (nZIF-7) were blended with poly(ether imide) (PEI) to fabricate a new mixed-matrix membrane (nZIF-7/PEI). nZIF-7 was chosen in order to demonstrate the power of postsynthetic modification (PSM) by linker exchange of benzimidazolate to benzotriazolate for tuning the permeability and selectivity properties of a resulting membrane (PSM-nZIF-7/PEI). These two new membranes were subjected to constant volume, variable pressure gas permeation measurements (H_2, N_2, O_2, CH_4, CO_2, C_2H_6, and C_3H_8), in which unique gas separation behavior was observed when compared to the pure PEI membrane. Specifically, the nZIF-7/PEI membrane exhibited the highest selectivities for CO_2/CH_4, CO_2/C_2H_6, and CO_2/C_3H_8 gas pairs. Furthermore, PSM-nZIF-7/PEI membrane displayed the highest permeabilities, which resulted in H_2/CH_4, N_2/CH_4, and H_2/CO_2 permselectivities that are remarkably well-positioned on the Robeson upper bound curves, thus, indicating its potential applicability for use in practical gas purifications.

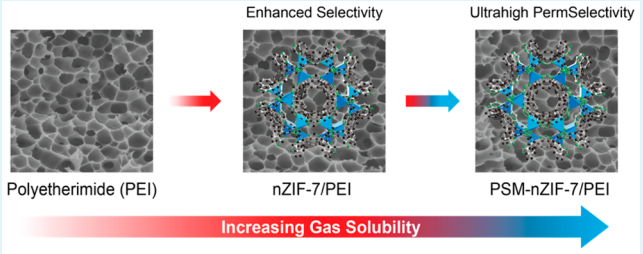

KEYWORDS: *metal−organic frameworks, mixed-matrix membranes, gas separation, nanomaterials, zeolitic imidazolate frameworks*

1. INTRODUCTION

Membranes for gas separation processes are becoming increasingly important for their potential in reducing energy requirements, as well as the operation and infrastructure costs.[1−6] Polymers are useful as membranes because they can be processed into different forms and have the flexibility to withstand operational stress.[7,8] Control of the permeability and selectivity within such membranes and correlating these parameters with the underlying molecular structure of the polymer represent some of the key challenges in the field.[7,8] To address these challenges, mixed-matrix membranes (MMMs), where porous inorganic nanoparticles are embedded within a polymer to introduce openness in an otherwise dense matrix, is a promising approach.[1,9−12] In this context, being able to use porous nanoparticles that are amenable to functionalization by changing the electronic and steric character of their constituents is paramount. Accordingly, nanocrystals of zeolitic imidazolate frameworks (nZIFs) are potentially ideal materials to serve as components in the MMMs.[13−25] nZIFs are metal−organic structures based on zeolite topologies, where the metal and the organic (imidazolates) components can be varied and, especially for the imidazolates, precisely functionalized without changing the topology of the overall structure.[26−28] An additional advantage to ZIFs is that they blend relatively well with organic polymers and, therefore, can be homogeneously mixed within the matrix.[13−25]

In this contribution, we use nZIF-7[29] blended with poly(ether imide) (PEI) as a means to tune the performance of a MMM and demonstrate how the postsynthetic exchange of benzimidazolate to benzotriazolate can modulate or enhance simultaneously both the permeability and selectivity properties (Scheme 1). Specifically, three membranes were fabricated: pure PEI membrane (PEI), nZIF-7 blended with PEI (nZIF-7/PEI), and postsynthetic modification (PSM) by linker exchange with

Special Issue: Hupp 60th Birthday Forum

Received: December 9, 2016
Accepted: January 18, 2017
Published: January 31, 2017

DOI: 10.1021/acsami.6b15803
ACS Appl. Mater. Interfaces 2017, 9, 33401−33407

Scheme 1. (A) Single Crystal X-ray Structure of ZIF-7 (also Structure of nZIF-7); (B) Postsynthetic Modified PSM-nZIF-7[a]

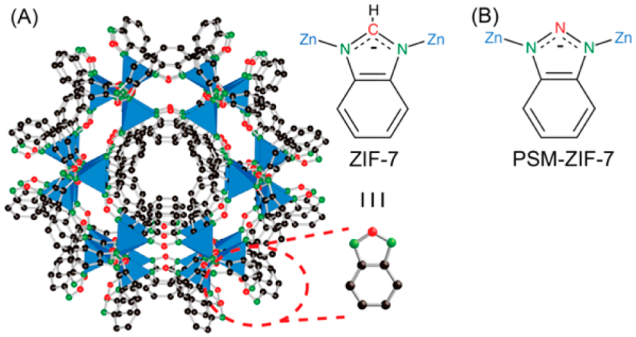

[a]These were blended in polyetherimide-based (PEI) mixed-matrix membranes. The opening of the accessible six-membered window leading to a large sodalite cage, characteristic of the **sod** topology, is displayed. Atom colors: C, black; N, green; Zn, blue tetrahedra. H atoms are omitted for clarity. Red atoms distinguish whether there is either a C atom as in nZIF-7 (A) or a N atom as in PSM-nZIF-7 (B).

benzotriazolate nZIF-7 blended with PEI (PSM-nZIF-7/PEI). These MMMs were produced for the first time, and their textural properties were characterized. Following this, all three materials were subjected to constant volume, variable pressure (CV/VP) gas permeation measurements in order to analyze their gas separation properties. Accordingly, we found that the gas transport behavior through the membrane was tunable from a dominant diffusion-based mechanism for the pure PEI membrane to a dominant solubility-driven mechanism for the ZIF-based MMMs. This is supported by the fact that the CO_2/N_2 selectivity experienced a 4-fold improvement when using the nZIF-7/PEI membrane in comparison to the pure PEI membrane (3.8 and 16.8 for the pure PEI and nZIF-7/PEI membranes, respectively), while the H_2/CO_2 selectivity drastically reduced by 3-fold (10.4 and 3.2 for the pure PEI and nZIF-7/PEI membranes, respectively). Furthermore, improved permeabilities for CO_2 (246 barrer) and H_2 (2021 barrer) were observed for the nitrogen-rich PSM-nZIF-7/PEI membrane due to the higher solubility of all gases that were tested. Finally, we report the unprecedented H_2/CH_4, N_2/CH_4, and H_2/CO_2 permselectivities for PSM-nZIF-7/PEI, which highlights this material's potential for gas purification.[8]

2. EXPERIMENTAL SECTION

2.1. Materials and General Procedures. All reagents were used as received without further purification. Zinc nitrate hexahydrate (≥99% purity, $Zn(NO_3)_2{\cdot}6H_2O$) was purchased from Loba, Mumbai, India. Benzimidazole (≥99% purity) and benzotriazole (≥99% purity) were purchased from Alfa Aeser. *N*,*N*′-Dimethylformamide (≥99.5% purity, DMF) and methanol (≥99.9% purity) were purchased from Scharlau. *N*,*N*′-Dimethylacetamide (≥99% purity, DMA), deuterated dimethyl sulfoxide (99.9%, DMSO-d_6), and deuterium chloride (35% DCl in D_2O) were purchased from Aldrich Chemical Co. Poly(ether imide) (PEI; Sabic Ultem 1000), H_2 (99.999%), CH_4 (99.9%), C_2H_6 (99.9%), and C_3H_8 (99.9%) were purchased form Abdullah Hashem Industrial Gas Co., Jeddah, Saudi Arabia. CO_2 (99.9%), N_2 (99.999%), and O_2 (99.9%) were purchased from Air Liquide, Dammam, Saudi Arabia.

Powder X-ray diffraction (PXRD) patterns were collected on a Bruker D8 Advance employing Ni-filtered Cu Kα radiation (λ = 1.54178 Å). ^{1}H and ^{13}C nuclear magnetic resonance (NMR) spectroscopy measurements were carried out using a JEOL JNM-LA500 spectrometer at 500 and 125.6 MHz, respectively. All chemical shifts were referenced relative to trimethylsilane. Fourier transform infrared (FT-IR) spectroscopy was performed using a Nicolet NXR FT−Raman spectrometer with a single reflection Diamond plate. Field emission scanning electron microscopy (SEM) analysis was performed using gold sputtered samples on a TESCAN MIRA3 (10−30 kV accelerating voltage) with energy-dispersive X-ray spectroscopy (EDX) analysis measured using an Oxford Instruments X-Max^N silicon drift detector. Thermogravimetric analysis (TGA) was conducted using a TA Q500 with the sample held in a platinum pan under airflow.

2.2. Synthesis of Nanozeolitic Imidazolate Framework-7 (nZIF-7).[3] $Zn(NO_3)_2{\cdot}6H_2O$ (1.25 g, 4.2 mmol) and benzimidazole (1.54 g, 13 mmol) were dissolved separately in 100 mL of DMF. Once dissolved, the two solutions were mixed in a round-bottom flask, which was continuously stirred for 72 h at 35 °C. After the elapsed time, crystalline nZIF-7 was obtained in 70% yield and subsequently separated by centrifugation at 6,000 rpm for 20 min. The mother liquid was discarded, and the resulting white powder was washed with methanol (3 × ∼50 mL). nZIF-7 was then dried at 90 °C for 12 h. FT-IR (400−4000 cm^{-1}): 3456 (br), 3056 (m), 2922 (w), 1776 (w), 1674 (s), 1609 (m), and 742 (s).

2.3. Postsynthetic Modification by Linker Exchange of nZIF-7 (PSM-nZIF-7).[30] nZIF-7 particles were suspended in a 50 mL methanol solution of benzotriazole (100 mg mL^{-1}). The resulting mixture was heated with stirring for 24 h. The benzotriazole solution was refreshed with a new benzotriazole solution, having the same concentration, after 24 h for a total of 3 days. The linker exchange process was monitored by ^{1}H and ^{13}C NMR spectroscopies. Prior to the NMR measurement, the solid was washed with methanol (10 × ∼2 mL) and dried at 120 °C for 12 h. The dried solid (∼10 mg) was digested by 50 μL of DCl, and 500 μL of DMSO-d_6 was added once the solid was dissolved. FT-IR (4000−4000 cm^{-1}): 3058 (br), 2922 (w), 1677 (w), 1610 (w), 1478 (s), 1226 (s), 1175 (m), and 744 (s).

2.4. Preparation of Poly(ether imide) and Mixed-Matrix Membrane. In a typical procedure, a 20 wt % PEI solution was prepared by mixing PEI (0.63 g) with DMA (2.5 mL) at 45 °C. The resulting mixture was stirred under vacuum for 24 h until PEI completely dissolved. The homogeneous solution was cast on a glass plate, with the aid of a casting knife at 400 μm thickness, and then allowed to coagulate under ambient conditions. For the preparation of nZIF-7/PEI and PSM-nZIF-7/PEI membranes, 33 mg of nZIF-7 or PSM-nZIF-7 was first solvent-exchanged with DMA to replace all of the methanol and then these solvent-exchanged nanoparticles were mixed with the aforementioned PEI solution after 18 h. Stirring was resumed for another 6 h at 45 °C under vacuum. These mixtures were cast (300 μm thickness) and coagulated, the same as that described for the PEI membrane. After coagulation, all membranes were left to dry overnight. DMA was exchanged from the pure PEI membrane and the MMMs by immersing each of the membranes separately in methanol (10 mL, 2×/day for 3 days). Finally, the membranes were dried at 100 °C for 18 h.

2.5. Single Gas Permeation Measurements. An in-house constant volume, variable pressure (CV/VP) apparatus was used to measure the pure gas permeability by time-lag analysis. A permeation cell (Millipore high pressure 316 stainless filter holder, 25 mm) was used to mount and seal the membranes from leaks using O-ring compression. Prior to each run, the entire apparatus was evacuated under reduced pressure (35 mTorr) at 35 °C. This process occurred while monitoring the rate of downstream, steady-state pressure. A successful leak-free system was concluded when the off-gassing was <1% of the rate of steady-state pressure rise compared to penetrant gas. All pure gas experiments were run at a feed pressure of 1520 Torr (2.03 bar). The downstream pressure rise during a permeation measurement was monitored using an 8 Torr Pfeiffer transducer. The permeation experiment was continued for a total time of at least 10 times the time lag. Upon completion of a single CV/VP gas permeation measurement, the sample cell was re-evacuated to the initial pressure to proceed forward to the next gas analyzed. All single gas measurements were carried out three times in order to ensure reproducibility and to confirm the absence of any residual gas from the previous run.

DOI: 10.1021/acsami.6b15803
ACS Appl. Mater. Interfaces 2017, 9, 33401−33407

3. RESULTS AND DISCUSSION

3.1. Synthesis and Characterization of nZIF-7, PSM-nZIF-7, and Their Mixed-Matrix Membranes. To gain insight into the ease of tuning a mixed-matrix membrane's permeability and selectivity properties, a design strategy was implemented using nZIF-7, which is amenable to pore environment modification, to blend with PEI as the platform matrix polymer. Postsynthetic modification of nZIF-7 by linker exchange of benzimidazolate with benzotriazolate was chosen in order to introduce additional polar atoms within the internal pore environment.[30−34] The subsequent blending of PSM-nZIF-7 in a PEI-based MMM, when compared to the original nZIF-7/PEI membrane, is a rational strategy, since the thermodynamic affinity (i.e., solubility) of gases generally increases upon a greater presence of polar atoms within the internal pores, thus leading to an overall enhancement in permeation.[35]

Accordingly, the synthesis of nZIF-7 was developed with modifications to a previously reported procedure with nanocrystalline powders being obtained in 70% yield.[30] Prior to structural analysis, nZIF-7 powder was thoroughly washed with DMF and methanol, followed by activation to remove any unreacted species and occluded guest molecules, respectively. The structure of nZIF-7 was confirmed by powder X-ray diffraction analysis (PXRD), in which the as-synthesized and activated samples' diffraction patterns were in agreement with the pattern simulated from the reported crystal structure of ZIF-7 (see Supporting Information section S1). The nZIF-7 particle size and uniformity were assessed by scanning electron microscopy (SEM) measurements. From the SEM images, nZIF-7 crystallites were clearly observed having a uniform morphology with a narrow size dispersity of 40−70 nm (Figure 1A and SI Figure S2).

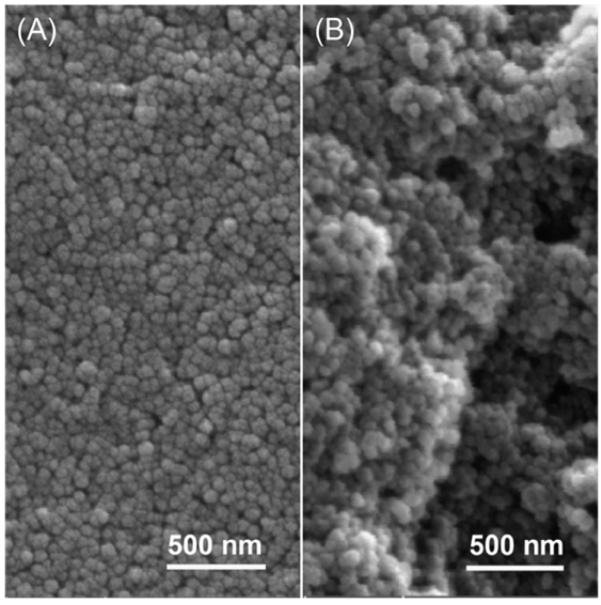

Figure 1. Scanning electron microscopy (SEM) images of nZIF-7 (A) and PSM-nZIF-7 (B) nanoparticles showing their size and shape uniformity.

The procedure for the PSM by linker exchange of nZIF-7 was also adopted with modification from a previous report.[30] The crystallinity and phase purity of PSM-nZIF-7 were confirmed by PXRD analysis, in which correspondence was observed when comparing the diffraction pattern with that of nZIF-7 (SI Figure S3). The success of the exchange was confirmed and quantified by ^{1}H and ^{13}C NMR analysis. In a typical NMR experiment, after a preset reaction time had elapsed, an aliquot of PSM-nZIF-7 product was separated and thoroughly washed with methanol (at least 10 times) in order to ensure there were no unreacted benzotriazole linkers remaining within the pores. After washing, PSM-nZIF-7 crystals were dried and subsequently digested using DCl/DMSO-d_6, which led to a linker exchange of up to 61% being observed (SI Figures S5−S8). SEM analysis was also employed to demonstrate that the particle size and homogeneous morphology of PSM-nZIF-7 was retained (Figure 1B and SI Figure S9).

Prior to the preparation of mixed-matrix membranes, the porosities and thermal stabilities of both nZIF-7 and PSM-nZIF-7 were analyzed by N_2 adsorption isotherms at 77 K and thermogravimetric analysis (TGA), respectively. Accordingly, the Brunauer−Emmett−Teller (BET) and Langmuir surface areas satisfactorily agreed with the values previously reported.[30] Specifically, the BET (Langmuir) surface area of nZIF-7 was calculated to be 350 (485) $m^2\ g^{-1}$ as compared with 360 (480) $m^2\ g^{-1}$ reported for ZIF-7 (SI Figure S11).[36,37] Similarly, the BET (Langmuir) surface area for PSM-nZIF-7 was found to be 290 (410) $m^2\ g^{-1}$, which was higher than previously reported (BET, 210 $m^2\ g^{-1}$) (SI Figure S12).[30] The latter results clearly indicate that nZIF-7 retains its porosity upon PSM linker exchange. It is noted that the observed hysteresis upon desorption is well-known to occur for ZIF-7 as there exists a gate opening effect resulting from the free rotation of the benzimidazolate linker being fixed by the neighboring Zn^{2+} sites.[36,37] TGA measurements of nZIF-7 and PSM-nZIF-7 exhibited thermal decompositions occurring at 460 and 430 °C, respectively, thus demonstrating the two structures' architecturally robust properties (SI Figure S13).

After successful synthesis and characterization of nZIF-7 and PSM-nZIF-7, MMMs were prepared with PEI functioning as the matrix. In a typical procedure, methanol-exchanged nZIF-7 or PSM-nZIF-7 nanoparticles were first suspended in *N*,*N*-dimethylacetamide (DMA) solvent in order to replace the methanol. A PEI solution in DMA was then prepared and stirred under vacuum at 45 °C for 18 h in order to completely dissolve the PEI. At this point, the DMA-exchanged nZIF-7 or PSM-nZIF-7 was suspended within the PEI solution to afford a final concentration of 20 wt % PEI with respect to DMA and a 5 wt % loading of the appropriate nZIF. This concentration and loading were chosen in order to obtain a solution density that was suitable for casting a final MMM with enough mechanical stability under the prescribed working pressure and to avoid the formation of defects within the resulting MMM, respectively. Casting of the nZIF-7/PEI and PSM-nZIF-7/PEI solutions took place with the aid of a casting knife. The MMMs were then solvent-exchanged with methanol and activated at 100 °C for 18 h prior to further structural characterization.

The textural properties of the MMMs were analyzed by SEM, in which both MMMs exhibited the formation of unique, sponge-like structures (Figure 2 and SI Figure S14). When compared to commonly reported dense membranes, this sponge-like structural feature is advantageous in that it allows for high flux permeation as well as the ability to perform multistage separation processes across one membrane.[38,39] High degrees of dispersity of nZIF-7 and PSM-nZIF-7 throughout the MMMs was proven by energy-dispersive X-ray spectroscopy (EDX) analysis on both the surface and cross-section of each MMM (SI, Figures S15−S19). Furthermore, the EDX-derived elemental

DOI: 10.1021/acsami.6b15803
ACS Appl. Mater. Interfaces 2017, 9, 33401−33407

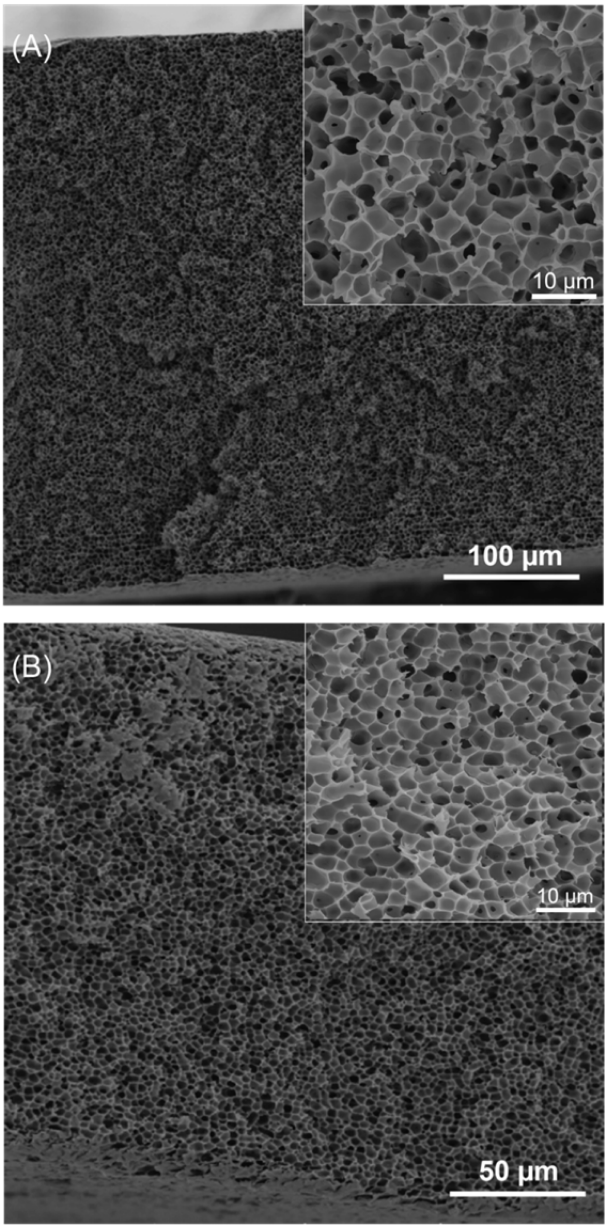

Figure 2. SEM images of the cross-sections of the PEI membrane (A) and 5 wt % nZIF-7/PEI membrane (B). The insets depict the sponge-like features of the membranes upon magnification.

mapping demonstrated that zinc, indicative of the presence of the respective ZIF, was widely dispersed throughout the entirety of both MMMs (SI Figures S20 and S21).

3.2. Gas Permeation Measurements. To assess and compare the permeation properties of the pure PEI membrane with the nZIF-7/PEI and PSM-nZIF-7/PEI membranes, CV/VP gas permeation measurements were performed (SI section S3). Accordingly, each of these samples were separately loaded into a permeation cell. Residual solvents were completely removed from the pure PEI membrane and the MMMs by evacuating the samples loaded in the permeation cell in situ at 35 °C for ~24 h. Once the cells were determined to be leak-free, CV/VP single gas permeation measurements were executed using H_2, O_2, N_2, CO_2, CH_4, C_2H_6, and C_3H_8 gas. Typically, upon halting the evacuation of the permeation cell, an upstream pressure of 1520 Torr (2.03 bar) was applied using the appropriate gas. Consecutively, the rise in downstream pressure for each gas permeation test was recorded as a function of time. A steady state was finally declared for the gas permeation once there was a constant slope of permeate pressure (SI Figure S23). The O_2/N_2 selectivity was always higher than the Knudsen diffusion selectivity (5.5, 4.2, and 1.5 versus. 1.1 for the pure PEI, nZIF-7/PEI, and PSM-nZIF-7/PEI versus Knudsen diffusion selectivity, respectively), which, in conjunction with the time lag recorded for each gas, represents a confirmation of the membrane reliability.[25]

Permeability Trends. The permeability obtained from the CV/VP single gas permeation measurements are summarized in Table 1 and, in general, follow the increasing trend of nZIF-7/PEI < PEI < PSM-nZIF-7/PEI membranes. From the permeability data, it is clear that a sharp maximum permeability for H_2 was observed in both the pure PEI membrane (856.1 barrer) and in the MMMs (207.0 and 2020.9 barrer for nZIF-7/PEI and PSM-nZIF-7/PEI membranes, respectively) when compared to all other tested gases (Figure 3, Table 1). By blending nZIF-7 in PEI, there was a significant decrease in the permeability for all gases analyzed when compared with those observed for the pure PEI membrane. Despite this decrease, the CO_2 permeability was observed to be less affected than

Table 1. Permeability of Pure PEI Membrane and nZIF-7/PEI and PSM-nZIF-7/PEI MMMs

	permeability (barrer)[a]		
gas	PEI	nZIF-7/PEI	PSM-nZIF-7/PEI
H_2	856.1	207.0	2020.9
CO_2	82.5	64.7	245.9
O_2	119.9	15.9	272.9
N_2	21.8	3.8	182.6
CH_4	18.9	5.0	107.9
C_2H_6	18.9	3.2	73.3
C_3H_8	18.3	3.0	45.5

[a]Conditions for the CV/VP single gas permeation measurements: pre-evacuation at 35 °C followed by the introduction of an upstream pressure of 1520 Torr (2.03 bar) for each single gas measured. One barrer = 10^{-10} $(cm^3(STP)\ cm)/(cm^2\ s\ cmHg)$.

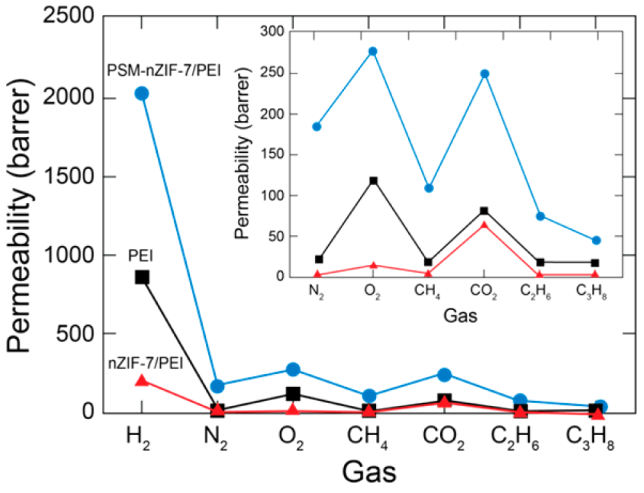

Figure 3. Constant volume, variable pressure (CV/VP) single gas permeation of different gases (H_2, N_2, O_2, CH_4, CO_2, C_2H_6, and C_3H_8) on a pure PEI membrane (black squares) in comparison to nZIF-7/PEI (red triangles) and PSM-nZIF-7/PEI (blue circles) MMMs. The inset depicts the permeability of N_2 to C_3H_8.

DOI: 10.1021/acsami.6b15803
ACS Appl. Mater. Interfaces 2017, 9, 33401−33407

the other gases studied. On the other hand, PSM-nZIF-7 blended in PEI led to an enhancement in permeability of all tested gases compared to the pure PEI membrane. For example, the permeability of H_2 (2020.9 barrer) and CO_2 (245.9 barrer) increased by factors of 2.4 and 3, respectively, for PSM-nZIF-7/PEI in comparison to the pure PEI. As expected, we note that the unique permeability trends are not only a result of the molecular sieving effect, which has been found for other ZIF-based MMMs.[14] In those cases, the permeability would be expected to follow the trend of H_2 (2.89 Å) > CO_2 (3.3 Å) > O_2 (3.46 Å) > N_2 (3.6 Å) > CH_4 (3.8 Å) > C_2H_6 (3.9 Å) > C_3H_8 (5.12 Å). The fact that it does not for our membranes reveals that the permeability is based upon more than simple diffusivity.

Comparison of Ideal Selectivity. The sharp maximum permeability for H_2 resulted in H_2/O_2, H_2/CO_2, H_2/CH_4, H_2/C_2H_6, and H_2/C_3H_8 gas pair ideal selectivities for the pure PEI membrane of 7.1, 10.4, 46.6, 45.4, and 46.8, respectively (Table 2). Despite the observed decrease in overall permeability,

Table 2. Ideal Selectivity (α) of Pure PEI Membrane and nZIF-7/PEI and PSM-nZIF-7/PEI MMMs

	α^a		
gas pair	PEI	nZIF-7/PEI	PSM-nZIF-7/PEI
O_2/N_2	5.5	4.2	1.5
H_2/O_2	7.1	13.0	7.4
H_2/N_2	39.2	53.9	11.1
H_2/CO_2	10.4	3.2	8.2
H_2/CH_4	46.6	41.8	18.7
H_2/C_2H_6	45.4	64.9	27.6
H_2/C_3H_8	46.8	69.0	46.3
CO_2/O_2	0.7	4.1	0.9
CO_2/N_2	3.8	16.8	1.3
CO_2/CH_4	4.5	13.1	2.3
CO_2/C_2H_6	4.4	20.3	3.4
CO_2/C_3H_8	4.5	21.6	5.6
N_2/CH_4	1.15	0.76	1.69

[a]Permeability ratio of the gas with the higher permeation relative to the gas with the lower.

the nZIF-7/PEI membrane demonstrated a remarkable enhancement in selectivity for the H_2/O_2, H_2/C_2H_6, and H_2/C_3H_8 gas pairs (13.0, 64.9, and 69.0, respectively, Table 2) when compared to the pure PEI membrane. Although the H_2/CO_2 gas pair selectivity (3.2) was negatively impacted by the low CO_2 permeability, there was a substantially higher calculated CO_2/N_2 gas pair selectivity (16.8) when compared with those found for the pure PEI membrane (10.4 for H_2/CO_2 and 3.8 for CO_2/N_2, respectively). Furthermore, nZIF-7/PEI membrane's selectivity toward CO_2 over all other measured hydrocarbon gases was highlighted by ideal selectivity values of 13.1 (4.5), 20.3 (4.4), and 21.6 (4.5) for CO_2/CH_4, CO_2/C_2H_6, and CO_2/C_3H_8 for nZIF-7/PEI (pure PEI), respectively (Table 2). We attribute the increase of nZIF-7/PEI membrane's remarkable CO_2/hydrocarbon and CO_2/N_2 gas pair selectivity to a noticeable decrease in hydrocarbon and N_2 permeation through the nZIF-7 particles embedded within the PEI membrane (Figure 3).

PermSelectivity. Although ideal selectivity is a useful measure for displaying the preferential permeation of different gases through a specific membrane, we refer to permselectivity as a method for evaluating the overall performance of membranes for practical gas separation processes. Indeed, permselectivity is a comparison of a material's ideal selectivity and permeability properties together for different gas systems. Accordingly, the increased permeability of H_2, CO_2, and CH_4 for PSM-nZIF-7/PEI led to an unprecedented permselectivity of H_2/CH_4 and H_2/CO_2 (18.7 and 8.2 selectivities, respectively, with a H_2 permeability of 2020.9 barrer), which surpasses the present (2008) Robeson upper bound curve (SI Figures S27 and S28).[8] Furthermore, in general, the comparison of the CO_2/CH_4, CO_2/N_2, and N_2/CH_4 permselectivity with the upper bound curves demonstrated improvement when nZIF-7 or PSM-nZIF-7 was blended with PEI (Figure 4 and SI Figures S27–S30).

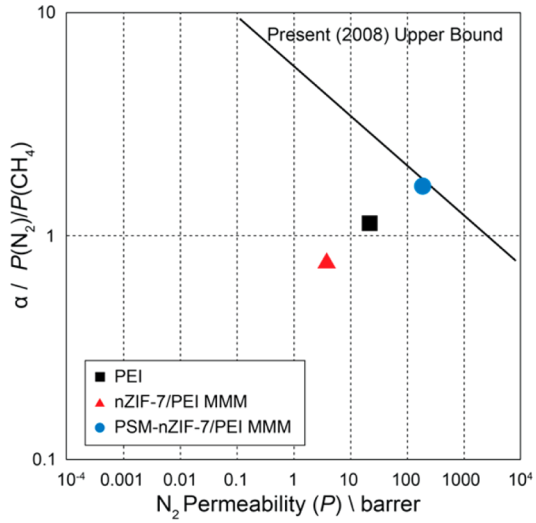

Figure 4. Relationship between N_2 permeability (P) and N_2/CH_4 gas pair selectivity (α) in comparison with the Robeson upper bound curve[7] for pure PEI membrane (black square), nZIF-7/PEI MMM (red triangle), and PSM-nZIF-7/PEI MMM (blue circle).

Gas Transport Mechanism. The gas transport behavior through the pure PEI membrane as well as that of the nZIF-7/PEI and PSM-nZIF-7/PEI MMMs was evaluated based on the solution-diffusion model.[40] This model is widely applied to polymeric membranes, in which gas permeability (P) is established as the product of the diffusion (D) and solubility (S) coefficients.[40] Specifically, the diffusion coefficient reflects the kinetic transport of a gas molecule through the respective membrane. This is correlated with the molecular size of the gas, which is expressed here as the Lennard-Jones diameter. D can be derived experimentally from the time lag, θ (s), and membrane thickness, l (cm), as $D = l^2/6\theta$ (SI section S3). The solubility coefficient, S, reflects the membranes' interactions with the gases, which can be correlated with the gas' normal boiling point. Upon calculating the experimentally derived P and D, a facile calculation leads to the solubility coefficient, S.[40]

In general, nZIF-7/PEI and PSM-nZIF-7/PEI MMMs exhibit a substantial decrease in diffusivity from H_2 to C_3H_8, whereas the solubility increased when both are compared to that of the pure PEI membrane (Figure 5). As shown in Figure 5A, gas molecules with larger diameters experience more resistance to diffusion (i.e., lower diffusivity) through the pure PEI membrane than they do with either of the MMMs. This results in a diffusivity trend of PEI > PSM-nZIF-7/PEI > nZIF-7/PEI, with PEI displaying the highest diffusivities for all gases tested.

DOI: 10.1021/acsami.6b15803
ACS Appl. Mater. Interfaces 2017, 9, 33401–33407

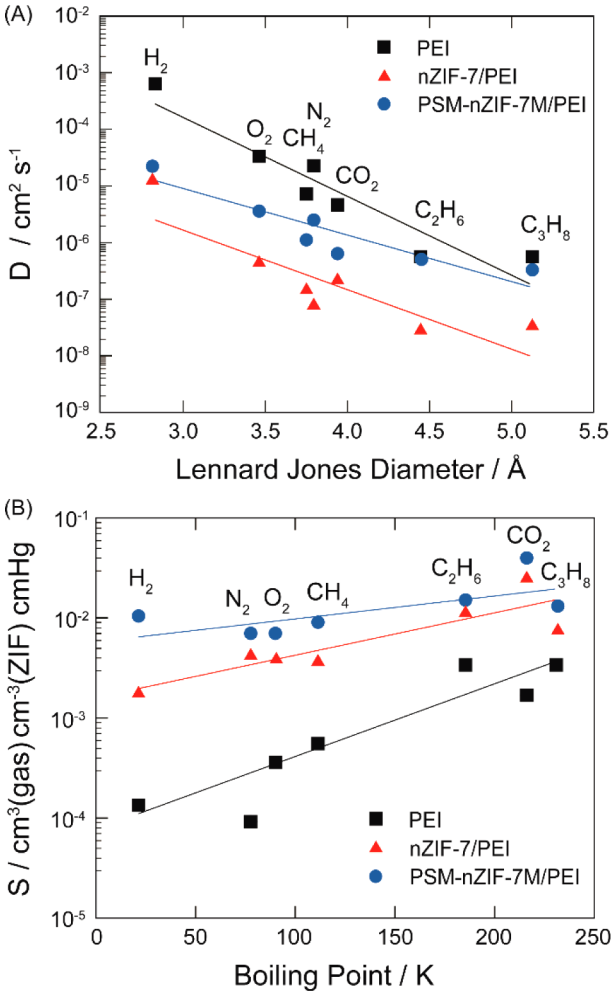

Figure 5. (A) Diffusion coefficients (D) versus Lennard-Jones diameter and (B) solubility coefficients (S) versus normal boiling point at 2 bar for PEI (black), nZIF-7/PEI MMM (red), and PSM-nZIF-7/PEI MMM (blue).

It is noted that at the operating temperature (35 °C), when a ZIF material is present in a PEI-based matrix, the membrane is expected to solidify and experience a decrease in the degree of flexibility, thus leading to lower diffusivities.[19] In terms of solubility, there was an increasing trend observed for the MMMs in direct relation to the normal boiling point of the gases (Figure 5B).

These findings are in agreement with the solution-diffusion mechanism for permeation. The enhanced solubility trend of PEI < nZIF-7/PEI < PSM-nZIF-7/PEI is expected as the latter MMM incorporates an extra polar nitrogen atom within the ZIF's backbone structure. This inevitably increases the thermodynamic affinity of polarizable gases such as CO_2 (Figure 5B). It is noted that, in the presence of either ZIF nanoparticles, not all gases are affected similarly in terms of diffusivity and solubility. For example, H_2 was observed to have a 27-fold decrease in diffusivity, yet experienced a 76-fold increase in solubility on the PSM-nZIF-7/PEI membrane when compared to the pure PEI membrane. On the other hand, CO_2 was shown to only have an 8-fold lower diffusivity and 23-fold higher solubility under the same comparison (SI Tables S1−S3).

4. CONCLUSION

We presented for the first time the synthesis of nZIF-7/PEI and its postsynthetic modified PSM-nZIF-7/PEI MMM and evaluated the resulting changes in the gas separation properties of these materials. Use of nZIF-7 and PSM-nZIF-7 blended within PEI matrix led to unique behavior with respect to gas permeation: the permeability of all gases tested (H_2, N_2, O_2, CH_4, CO_2, C_2H_6, and C_3H_8) was highest for the PSM-nZIF-7/PEI MMM. On the other hand, although nZIF-7/PEI MMM exhibited the lowest permeabilities, the ideal selectivities for CO_2/CH_4, CO_2/C_2H_6, and CO_2/C_3H_8 were remarkably enhanced when compared to the pure PEI membrane or that of PSM-nZIF-7/PEI MMM. Furthermore, H_2/CH_4, N_2/CH_4, and H_2/CO_2 showed improved permselectivities of PSM-nZIF/PEI MMM compared to the present Robeson upper bound curve, indicating its potential for use in gas purification. As a result of these findings, this study demonstrated the power of postsynthetic modification on a ZIF structure for use in a MMM, in which one can sufficiently tune the interplay between the permeability and selectivity.

■ ASSOCIATED CONTENT

Supporting Information

The Supporting Information is available free of charge on the ACS Publications website at DOI: 10.1021/acsami.6b15803.

nZIF-7 and PSM-nZIF-7 characterization, including PXRD, TGA, N_2 sorption isotherms, and SEM and EDX images, and CV/VP single gas permeation experimental details (PDF)

■ AUTHOR INFORMATION

Corresponding Authors

*(B.A.A.M.) E-mail: bmayth@kfupm.edu.sa.
*(O.M.Y.) E-mail: yaghi@berkeley.edu.

ORCID

Mohamed A. M. Habib: 0000-0003-3459-1462
Omar M. Yaghi: 0000-0002-5611-3325

Notes

The authors declare no competing financial interest.

■ ACKNOWLEDGMENTS

We express appreciation to Dr. Hiroyasu Furukawa (Yaghi group, UC Berkeley) for valuable discussions. We gratefully acknowledge KFUPM and KACST-TIC on CCS for financial support (Project No. CCS-15). O.M.Y. and K.E.C. acknowledge the support of SAUDI ARAMCO, Saudi Arabia (Project No. ORCP2390).

■ DEDICATION

Dedicated to Professor Joseph T. Hupp on the occasion of his 60th birthday.

■ REFERENCES

(1) Seoane, B.; Coronas, J.; Gascon, I.; Benavides, M. E.; Karvan, O.; Caro, J.; Kapteijn, F.; Gascon, J. Metal-Organic Framework Based Mixed Matrix Membranes: A Solution for Highly Efficient CO_2 Capture? *Chem. Soc. Rev.* **2015**, *44*, 2421−2454.

(2) Anderson, M.; Wang, H.; Lin, Y. S. Inorganic Membranes for Carbon Dioxide and Nitrogen Separation. *Rev. Chem. Eng.* **2012**, *28*, 101−121.

(3) Denny, M. S., Jr.; Moreton, J. C.; Benz, L.; Cohen, S. M. Metal-Organic Frameworks for Membrane Based Separations. *Nat. Rev. Mater.* **2016**, *1*, 16078.

DOI: 10.1021/acsami.6b15803
ACS Appl. Mater. Interfaces 2017, 9, 33401−33407

(4) Qiu, S.; Xue, M.; Zhu, G. Metal-Organic Framework Membranes: From Synthesis to Separation Application. *Chem. Soc. Rev.* **2014**, *43*, 6116−6140.
(5) Venna, S. R.; Carreon, M. A. Metal-Organic Framework Membranes for Carbon Dioxide Separation. *Chem. Eng. Sci.* **2015**, *124*, 3−19.
(6) Shah, M.; McCarthy, M. C.; Sachdeva, S.; Lee, A. K.; Jeong, H.-K. Current Status of Metal-Organic Framework Membranes for Gas Separations: Promises and Challenges. *Ind. Eng. Chem. Res.* **2012**, *51*, 2179−2199.
(7) Baker, R. W. Future Directions of Membrane Gas Separation Technology. *Ind. Eng. Chem. Res.* **2002**, *41*, 1393−1411.
(8) Robeson, L. M. The Upper Bound Revisited. *J. Membr. Sci.* **2008**, *320*, 390−400.
(9) Zhang, Y.; Feng, X.; Yuan, S.; Zhou, J.; Wang, B. Challenges and Recent Advances in MOF-Polymer Composite Membranes for Gas Separation. *Inorg. Chem. Front.* **2016**, *3*, 896−909.
(10) Aroon, M. A.; Ismail, A. F.; Matsuura, T.; Montazer-Rahmati, M. M. Performance Studies of Mixed Matrix Membranes for Gas Separation - A Review. *Sep. Purif. Technol.* **2010**, *75*, 229−242.
(11) Chung, T.-S.; Jiang, L. Y.; Li, Y.; Kulprathipanja, S. Mixed Matrix Membranes (MMMs) Comprising Organic Polymers with Dispersed Inorganic Fillers for Gas Separation. *Prog. Polym. Sci.* **2007**, *32*, 483−507.
(12) Adams, R.; Carson, C.; Ward, J.; Tannenbaum, R.; Koros, W. Metal-Organic Framework Mixed Matrix Membranes for Gas Separations. *Microporous Mesoporous Mater.* **2010**, *131*, 13−20.
(13) Bae, T.-H.; Lee, J. S.; Qiu, W.; Koros, W. J.; Jones, C. W.; Nair, S. A High-Performance Gas-Separation Membrane Containing Submicrometer-Sized Metal-Organic Framework Crystals. *Angew. Chem., Int. Ed.* **2010**, *49*, 9863−9866.
(14) Wang, Z.; Wang, D.; Zhang, S.; Hu, L.; Jin, J. Interfacial Design of Mixed Matrix Membranes for Improved Gas Separation Performance. *Adv. Mater.* **2016**, *28*, 3399−3405.
(15) Zornoza, B.; Seoane, B.; Zamaro, J. M.; Tellez, C.; Coronas, J. Combination of MOFs and Zeolites for Mixed Matrix Membranes. *ChemPhysChem* **2011**, *12*, 2781−2785.
(16) Yang, T.; Xiao, Y.; Chung, T.-S. Poly-/Metal-Benzimidazole Nano-composite Membranes for Hydrogen Purification. *Energy Environ. Sci.* **2011**, *4*, 4171−4180.
(17) Song, Q.; Nataraj, S. K.; Roussenova, M. V.; Tan, J. C.; Hughes, D. J.; Li, W.; Bourgoin, P.; Alam, M. A.; Cheetham, A. K.; Al-Muhtaseb, S. A.; Sivaniah, E. Zeolitic Imidazolate Framework (ZIF-8) Based Polymer Nanocomposite Membranes for Gas Separation. *Energy Environ. Sci.* **2012**, *5*, 8359−8369.
(18) Wu, X.; Niknam Shahrak, M.; Yuan, B.; Deng, S. Synthesis and Characterization of Zeolitic Imidazolate Framework ZIF-7 for CO_2 and CH_4 Separation. *Microporous Mesoporous Mater.* **2014**, *190*, 189−196.
(19) Li, T.; Pan, Y.; Peinemann, K.-V.; Lai, Z. Carbon Dioxide Selective Mixed Matrix Composite Membrane Containing ZIF-7 Nano-Fillers. *J. Membr. Sci.* **2013**, *425−426*, 235−242.
(20) Yang, T.; Shi, G. M.; Chung, T.-S. Symmetric and Asymmetric Zeolitic Imidazolate Frameworks (ZIFs)/Polybenzimidazole (PBI) Nanocomposite Membranes for Hydrogen Purification at High Temperatures. *Adv. Energy Mater.* **2012**, *2*, 1358−1367.
(21) Yang, T. X.; Chung, T. S. Room-Temperature Synthesis of ZIF-90 Nanocrystals and the Derived Nano-Composite Membranes for Hydrogen Separation. *J. Mater. Chem. A* **2013**, *1*, 6081−6090.
(22) Nafisi, V.; Hagg, M. B. Development of Dual Layer ZIF-8/PEBAX-2533 Mixed Matrix Membrane for CO_2 Capture. *J. Membr. Sci.* **2014**, *459*, 244−255.
(23) Bhaskar, A.; Banerjee, R.; Kharul, U. ZIF-8@PBI-BuI Composite Membranes: Elegant Effects of PBI Structural Variations on Gas Permeation Performance. *J. Mater. Chem. A* **2014**, *2*, 12962−12967.
(24) Fang, M.; Wu, C.; Yang, Z.; Wang, T.; Xia, Y.; Li, J. ZIF-8/PDMS Mixed Matrix Membranes for Propane/Nitrogen Mixture Separation: Experimental Result and Permeation Model. *J. Membr. Sci.* **2015**, *474*, 103−113.
(25) Al-Maythalony, B. A.; Shekhah, O.; Swaidan, R.; Belmabkhout, Y.; Pinnau, I.; Eddaoudi, M. Quest for Anionic MOF Membranes: Continuous sod-ZMOF Membrane with CO_2 Adsorption-Driven Selectivity. *J. Am. Chem. Soc.* **2015**, *137*, 1754−1757.
(26) Eddaoudi, M.; Sava, D. F.; Eubank, J. F.; Adil, K.; Guillerm, V. Zeolite-like Metal-Organic Frameworks (ZMOFs): Design, Synthesis, and Properties. *Chem. Soc. Rev.* **2015**, *44*, 228−249.
(27) Nguyen, N. T. T.; Furukawa, H.; Gándara, F.; Nguyen, H. T.; Cordova, K. E.; Yaghi, O. M. Selective Capture of Carbon Dioxide under Humid Conditions by Hydrophobic Chabazite-type Zeolitic Imidazolate Frameworks. *Angew. Chem., Int. Ed.* **2014**, *53*, 10645−10648.
(28) Nguyen, N. T. T.; Lo, T. N. H.; Kim, J.; Nguyen, H. T. D.; Le, T. B.; Cordova, K. E.; Furukawa, H. Mixed-Metal Zeolitic Imidazolate Frameworks and their Selective Capture of Wet Carbon Dioxide over Methane. *Inorg. Chem.* **2016**, *55*, 6201−6207.
(29) Park, K. S.; Ni, Z.; Côté, A. P.; Choi, J. Y.; Huang, R.; Uribe-Romo, F. J.; Chae, H. K.; O'Keeffe, M.; Yaghi, O. M. Exceptional Chemical and Thermal Stability of Zeolitic Imidazolate Frameworks. *Proc. Natl. Acad. Sci. U. S. A.* **2006**, *103*, 10186−10191.
(30) Jiang, J.-Q.; Yang, C.-X.; Yan, X.-P. Postsynthetic Ligand Exchange for the Synthesis of Benzotriazole-containing Zeolitic Imidazolate Framework. *Chem. Commun.* **2015**, *51*, 6540−6543.
(31) Lalonde, M. B.; Mondloch, J. E.; Deria, P.; Sarjeant, A. A.; Al-Juaid, S. S.; Osman, O. I.; Farha, O. K.; Hupp, J. T. Selective Solvent-Assisted Linker Exchange (SALE) in a Series of Zeolitic Imidazolate Frameworks. *Inorg. Chem.* **2015**, *54*, 7142−7144.
(32) Karagiaridi, O.; Bury, W.; Sarjeant, A. A.; Stern, C. L.; Farha, O. K.; Hupp, J. T. Synthesis and Characterization of Isostructural Cadmium Zeolitic Imidazolate Frameworks via Solvent-Assisted Linker Exchange. *Chem. Sci.* **2012**, *3*, 3256−3260.
(33) Deria, P.; Mondloch, J. E.; Karagiaridi, O.; Bury, W.; Hupp, J. T.; Farha, O. K. Beyond Post-Synthetic Modification: Evolution of Metal-Organic Frameworks via Building Block Replacement. *Chem. Soc. Rev.* **2014**, *43*, 5896−5912.
(34) Zhu, H.; Wang, L.; Jie, X.; Liu, D.; Cao, Y. Improved Interfacial Affinity and CO_2 Separation Performance of Asymmetric Mixed Matrix Membranes by Incorporating Postmodified MIL-53(Al). *ACS Appl. Mater. Interfaces* **2016**, *8*, 22696−22704.
(35) Thirion, D.; Kwon, Y.; Rozyyev, V.; Byun, J.; Yavuz, C. T. Synthesis and Easy Functionalization of Highly Porous Networks through Exchangeable Fluorines for Target Specific Applications. *Chem. Mater.* **2016**, *28*, 5592−5595.
(36) Chen, D.-L.; Wang, N.; Wang, F.-F.; Xie, J.; Zhong, Y.; Zhu, W.; Johnson, J. K.; Krishna, R. Utilizing the Gate-Opening Mechanism in ZIF-7 for Adsorption Discrimination between N_2O and CO_2. *J. Phys. Chem. C* **2014**, *118*, 17831−17837.
(37) Zhao, P.; Lampronti, G. I.; Lloyd, G. O.; Suard, E.; Redfern, S. A. T. Direct Visualisation of Carbon Dioxide Adsorption in Gate-Opening Zeolitic Imidazolate Framework ZIF-7. *J. Mater. Chem. A* **2014**, *2*, 620−623.
(38) Hilal, N.; Ismail, A. F.; Wright, C. *Membrane Fabrication*; CRC Press: Boca Raton, FL, USA, 2015.
(39) Wang, Z.; Ma, J.; Liu, Q. Pure Sponge-like Membranes bearing both High Water Permeability and High Retention Capacity. *Desalination* **2011**, *278*, 141−149.
(40) Freeman, B., Yampolskii, Y., Pinnau, I., Eds. *Materials Science of Membranes for Gas and Vapor Separation*; John Wiley & Sons: Hoboken, NJ, USA, 2006.

DOI: 10.1021/acsami.6b15803
ACS Appl. Mater. Interfaces 2017, 9, 33401−33407